Critical dimensions in coherently strained coaxial nanowire heterostructures

S. Raychaudhuri and E. T. Yu[a)]
Department of Electrical and Computer Engineering, University of California, San Diego, La Jolla, California 92093-0407

(Received 16 October 2005; accepted 14 March 2006; published online 8 June 2006)

We present a methodology to determine critical dimensions for coherently strained coaxial nanowire heterostructures based on a well-known formalism used to determine the critical thickness in planar epitaxial growth. The unique geometry of the nanowire structure along with the volumetric similarity of the core and shell regions give rise to a number of possible stable core-shell configurations for a given choice of materials. We show that a unique critical core radius and critical shell thickness, dependent on core radius, can quantify these configurations. Illustrative calculations are presented for various nitride semiconductor-based core-shell structures. It is anticipated that this model will serve as a guide to determine the feasibility of specific coherently strained nanowire heterostructure designs. © *2006 American Institute of Physics*. [DOI: 10.1063/1.2202697]

I. INTRODUCTION

Recent successes in the growth and fabrication of semiconductor nanowires[1,2] have led to opportunities in device design for a variety of applications, including chemical and biological sensors,[3] field effect transistors,[4,5] laser diodes,[6,7] and light emitting diodes.[8,9] Many of these devices either require or can benefit from the use of heterostructures in their design, and nanowire heterostructures in both coaxial[5] and axial[10] geometries have been proposed to optimize device performance. In determining the feasibility of these designs it is necessary to consider the strain that arises in heterostructures due to the lattice mismatch between materials. Such strain not only affects the electronic and optical properties of the device but also determines the device dimensions at which coherence is lost and dislocations form, which will significantly alter or degrade device performance.

Only a limited amount of work has been done previously to model coherence and critical dimensions in nanowire structures. A model was developed recently to describe strain and coherence in axial nanowire heterostructures,[11] while the critical dimensions of isotropic coaxial structures[12] have been estimated by comparing the strain energy of two discrete states of the system. In this paper we provide a methodology for determining coherent geometries in coaxial nanowire heterostructures based on the formalism commonly used in thin film heteroepitaxy.[13,14] Illustrative calculations are presented for specific crystal structures and materials, but with some care the basic methods can be extended to any material system. This model is designed to provide a framework from which to determine the structural feasibility of various coherently strained core-shell nanowire structures.

II. ANALYTICAL FRAMEWORK

The geometry of the nanowire system considered is shown in Fig. 1. The nanowire consists of a core of radius r and shell of thickness h. Both regions possess the wurtzite crystal structure with the [0001] direction along the axis of the wire. The coherence requirement between the core and shell will result in cross-sectional and longitudinal strain components due to the mismatch in a-axis and c-axis lattice parameters, respectively. Both the cross-sectional strain and the longitudinal strain components must be considered when determining stable geometries for the system.

In this analysis we are interested in determining the dimensions at which coherence is lost. In planar thin film growth the typical limiting case is quantified using the "critical thickness," the film thickness at which the film is no longer coherent with the substrate due to strain relaxation via the formation of dislocations. A commonly used methodology to predict critical thickness examines the strain energy of the system and determines the film thickness at which it becomes energetically favorable to relieve lattice strain by inserting a dislocation.[13,14] In contrast to this case, the geometry of the coaxial nanowire along with the comparable volumes of the core and shell regions require that the dimensions of both the core and the shell be considered. This gives rise to the idea of critical dimensions: combinations of core and shell dimensions that will lead to stable, coherently strained structures.

In general it is found that the nanowire geometry is more forgiving than its thin film counterpart in that a number of dimensional choices exist to attain a stable coherent structure. For a given choice of materials there exists a critical core radius, below which the structure is always coherent regardless of shell thickness. Structures with a core radius greater than this critical value can still be stable provided

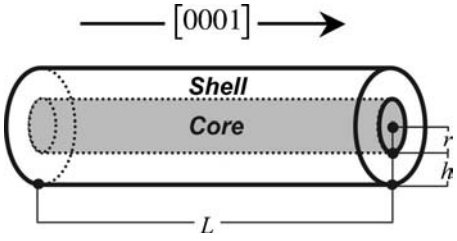

FIG. 1. Diagram of coaxial nanowire heterostructure and relevant geometric parameters.

[a)]Electronic mail: ety@ece.ucsd.edu

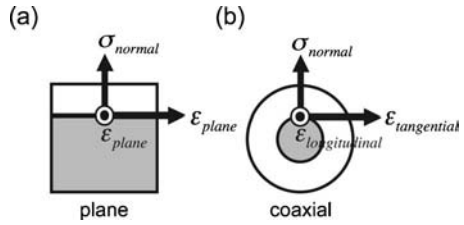

FIG. 2. Diagram of the orientation of stress (σ) and strain (ε) components in (a) planar heterostructures and (b) coaxial heterostructures.

that the shell thickness is below a critical shell thickness value. The critical shell thickness is dependent on the core radius, approaching the planar critical thickness as the core radius increases. The critical dimensions are found to be dependent only on core radius and shell thickness and have no dependence on the length of the wire.

A. Coherent strain energy calculation

Elastic theory and the well-known relations between stress and strain can be used to develop analytical expressions for strain energy in coaxial nanowire heterostructures. The nanowire structure is taken to be perfectly round with smooth surfaces and interfaces, thus neglecting any effects of faceting. This is done in order to apply a straightforward analytical approach to the problem and is not expected to significantly alter the calculation for sufficiently large structures. The derivation presented here is specific to wurtzite nanowires with the [0001] direction along the length of the wire. Analogous derivations can be carried out for other material systems provided that the elastic stiffness tensor is isotropic in the cross-sectional plane of the wire. If the cross section of the wire was anisotropic, it is likely that the shape of the wire would change to accommodate strain, thus violating assumptions used in this computation.

In planar thin film growth, the strain energy is calculated by assuming a number of geometric boundary conditions and using them to calculate the full strain field within the structure. The basic boundary conditions in planar thin film growth define two perpendicular in-plane strain components arising from lattice mismatch and a stress component normal to the interface, as shown in Fig. 2(a). In the coaxial nanowire geometry an analogous approach can be used, as illustrated in Fig. 2(b). At a single point on the cylindrical heterointerface, it is possible to define two perpendicular strain components due to lattice mismatch: one component along the length of the wire ($\varepsilon_{\text{longitudinal}}$) and the other tangential to the heterointerface ($\varepsilon_{\text{tangential}}$). The stress normal to the heterointerface, σ_{normal}, at that particular point is analogous to the stress in the growth direction in the planar case. Thus, by defining a Cartesian coordinate system comprised of longitudinal, tangential, and normal axes for a specific point on the nanowire heterointerface, it is possible to apply the planar formalism to solve for the full strain field at that point. By applying this approach to every point on the heterointerface, it is then possible to construct the full strain field within the system and subsequently to calculate the strain energy.

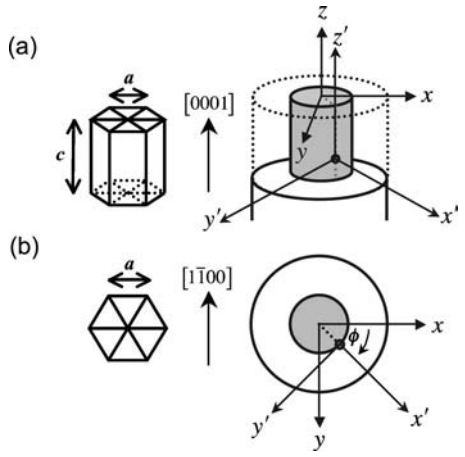

FIG. 3. (a) Cutaway and (b) cross-sectional diagrams of the coaxial nanowire structure and corresponding orientation of the wurtzite crystal geometry. $\{x,y,z\}$ denote the reference axes of the system while $\{x',y',z'\}$ denote the normal, tangential, and longitudinal axes for a specific point on the circular interface corresponding to the angle ϕ.

To implement this approach, it is necessary to specify an appropriately oriented Cartesian coordinate system for each point on the interface. This is accomplished by rotating the reference axes (denoted by x, y, and z) as shown in Fig. 3. If we specify a point on the interface at an angle ϕ relative to the reference axis x, the specific Cartesian axes for that point (denoted by x', y', and z') can be obtained by rotating the reference axes by an angle ϕ about the z axis. Longitudinal (z'), tangential (y'), and normal (x') boundary conditions, similar to those used in the planar formalism, can now be applied at that point on the interface.

Figure 3(a) shows the orientation of the wurtzite crystal structure relative to the coaxial wire geometry. From this diagram it is clear that longitudinal strain components will be imposed by the c-axis lattice mismatch between the core and shell materials. The longitudinal strain component in the core material is given by

$$f_c^{(i)} = \frac{c - c^{(i)}}{c^{(i)}}, \tag{1}$$

where c represents the strained lattice constant of the system and $c^{(i)}$ represents the unstrained lattice parameter of the core material. The longitudinal strain component in the shell material is given by

$$f_c^{(ii)} = \frac{c - c^{(ii)}}{c^{(ii)}}, \tag{2}$$

where $c^{(ii)}$ represents the unstrained lattice parameter of the shell material. In general, variables with superscripts (i) and (ii) will denote parameters specific to the core and shell materials, respectively.

Figure 3(b) shows the orientation of the wurtzite crystal structure relative to the cross section of the wire. The strain within the cross section is governed by a tangential lattice

mismatch strain component at each point on the heterointerface. In the core material, this strain component is given by

$$f_a^{(i)} = \frac{a - a^{(i)}}{a^{(i)}}, \tag{3}$$

where a represents the strained lattice constant of the system and $a^{(i)}$ represents the unstrained lattice parameter of the core material. Similarly, the tangential strain component in the shell material at a given point along the circular interface is given by

$$f_a^{(ii)} = \frac{a - a^{(ii)}}{a^{(ii)}}, \tag{4}$$

where $a^{(ii)}$ represents the unstrained lattice parameter of the shell material.

In planar thin film growth the top surface of the structure is unconstrained, allowing the film thickness to expand or contract as needed to accommodate strain. This can be expressed as a boundary condition that states that there will be no stress in the direction normal to the heterointerface.[13,14] In the coaxial nanowire geometry there is nothing constraining the outer surface of the nanowire system; thus the radius of the system is free to expand or contract in order to accommodate strain. For a particular point on the interface this yields the boundary condition that there will be no stress in the direction normal to the heterointerface at that point. The wire is assumed to be of infinite length and thus the effects of the circular faces at either end of the wire are not considered.

Using standard matrix notation[15] it is possible to write the elements of stress as a function of the strain and the elastic stiffness matrix for a given material.[15] These elements of stress and strain can then be rewritten in their tensor forms. Rotating these tensors about the z axis by an angle ϕ will yield expressions relating the normal, tangential, and longitudinal components of stress and strain for a given point on the interface, denoted by the angle ϕ. The normal, tangential, and longitudinal boundary conditions defined earlier can then be applied to elements of the rotated tensors as follows:

$$\sigma_1'(c_{ij}, \varepsilon_1, \varepsilon_2, \varepsilon_3, \varepsilon_6, \phi) = 0, \tag{5}$$

$$\varepsilon_2'(\varepsilon_1, \varepsilon_2, \varepsilon_6, \phi) = f_a, \tag{6}$$

$$\varepsilon_3' = \varepsilon_3 = f_c, \tag{7}$$

where σ_1' represents the rotated stress tensor element normal to the interface at a point specified by the angle ϕ, c_{ij} represents various elements of the elastic stiffness matrix of the material being considered, ε_i represents strain matrix elements relative to the reference axis, and ε_2' and ε_3' represent the rotated strain tensor elements tangential to the interface at the specified point and along the length of the wire at the specified point, respectively.

For planar growth it is also assumed that the strain components are perfectly perpendicular and that there are no shear strains that arise from lattice mismatch.[13,14] As in the planar case, for a single point on the heterointerface, there will be no shear strain components relative to the normal, tangential, and longitudinal directions. These conditions can be expressed as follows:

$$\varepsilon_4'(\varepsilon_4, \varepsilon_5, \phi) = 0, \tag{8}$$

$$\varepsilon_5'(\varepsilon_4, \varepsilon_5, \phi) = 0, \tag{9}$$

$$\varepsilon_6'(\varepsilon_1, \varepsilon_2, \varepsilon_6, \phi) = 0, \tag{10}$$

where ε_4', ε_5', and ε_6' represent the shear strain elements between the tangential and longitudinal axes, normal and longitudinal axes, and the normal and tangential axes, respectively.

From Eqs. (5)–(10) a complete solution for the strain field ε, can be obtained as a function of angular position ϕ. The resulting expression for the strain field can then be used to compute the strain energy density $w = \frac{1}{2} c_{ij} \varepsilon_i \varepsilon_j$, which when integrated over the volume of the material will yield an expression for the total strain energy.[15] The resulting expressions for strain energy U in the core and shell are then

$$U^{(i)} = \frac{[c_{11}^{(i)} f_a^{(i)}]^2 - [c_{12}^{(i)} f_a^{(i)} + c_{13}^{(i)} f_c^{(i)}]^2 + c_{11}^{(i)} f_c^{(i)} [c_{13}^{(i)} f_a^{(i)} + c_{33}^{(i)} f_c^{(i)}]^2}{2 c_{11}^{(i)}} L \pi (r^2), \tag{11}$$

$$U^{(ii)} = \frac{[c_{11}^{(ii)} f_a^{(ii)}]^2 - [c_{12}^{(ii)} f_a^{(ii)} + c_{13}^{(ii)} f_c^{(ii)}]^2 + c_{11}^{(ii)} f_c^{(ii)} [c_{13}^{(ii)} f_a^{(ii)} + c_{33}^{(ii)} f_c^{(ii)}]^2}{2 c_{11}^{(ii)}} L \pi [(r+h)^2 - r^2]. \tag{12}$$

Equations (11) and (12) are valid for wurtzite wires along the [0001] direction. A similar analysis utilizing the appropriate elastic stiffness tensor and lattice mismatch boundary conditions can be used to calculate the strain energy expressions for other material systems.

For a given geometry and material composition the equilibrium lattice constants of the strained system, a and c, will assume values that minimize the total strain energy of the system. We therefore seek to minimize $U_{\text{strain}} = U^{(i)} + U^{(ii)}$ with respect to a and c by using the strain expressions given in Eqs.(1)–(4). This minimization cannot be performed simultaneously for both a and c using analytical methods. Figure 4 shows values for a and c obtained by numerical minimization in a coaxial heterostructure with a 25 nm radius

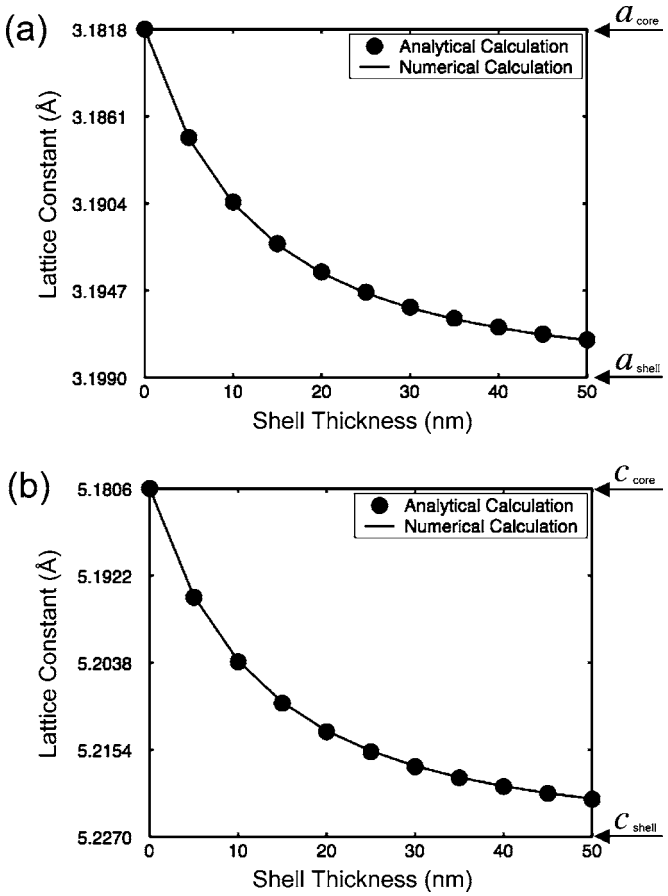

FIG. 4. Plot of the cross-sectional equilibrium lattice constants (a) a and (b) c as functions of shell thickness. The structure considered is comprised of a 25 nm GaN core and an $Al_{0.2}Ga_{0.8}N$ shell. The maximum and minimum y axis values on both plots are set to be the relaxed core and shell lattice constants, respectively.

GaN core, as a function of thickness of an $Al_{0.2}Ga_{0.8}N$ shell. The lattice constants and elastic stiffness constants used in the computation were taken from Ref. 16 and are all assumed to vary linearly with alloy composition.

The numerical results in Fig. 4 show that the equilibrium lattice constants will fall somewhere between the relaxed core and shell values and will tend toward those of the region with greater volume. This is expected given the direct relationship between strain energy and volume seen in Eqs. (11) and (12). These results show that for a given choice of material, geometry will determine the distribution of lattice strain between the core and shell materials. It is because of this that the dimensions of both core and shell must be considered in determining stable coherent geometries.

An analytical expression for the equilibrium lattice constant can provide a more intuitive understanding of how the core and shell dimensions affect the strain distribution between the two regions. From the numerical result it appears that the equilibrium lattice constants a and c have the same functional dependence on shell thickness when normalized to their respective relaxed core and shell lattice values, i.e.,

$$f_a^{(i)} = f_c^{(i)} = f^{(i)} = \frac{p - p^{(i)}}{p^{(i)}}, \tag{13}$$

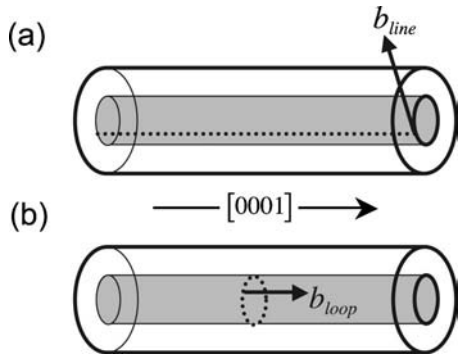

FIG. 5. (a) Orientation of an edge dislocation line along the [0001] direction with Burgers vector b_{line} in the $[11\bar{2}0]$ direction, tangential to the circular heterointerface. (b) Orientation of an edge dislocation loop in the cross-sectional plane of the wire with Burgers vector b_{loop} in the [0001] direction, along the length of the wire.

$$f_a^{(ii)} = f_c^{(ii)} = f^{(ii)} = \frac{p - p^{(ii)}}{p^{(ii)}}, \tag{14}$$

where p represents an equilibrium value for a generic lattice constant variable, $p^{(i)}$ represents the relaxed value of the corresponding generic core lattice constant, and $p^{(ii)}$ represents the relaxed value of a generic shell lattice constant. Substituting Eqs.(13) and (14) into U_{strain} and minimizing with respect to p yield

$$p = \frac{p^{(ii)}p^{(i)}[p^{(ii)}r^2\chi^{(i)} + p^{(i)}h(h+2r)\chi^{(ii)}]}{p^{(ii)}r^2\chi^{(i)} + p^{(i)}h(h+2r)\chi^{(ii)}}, \tag{15}$$

where $\chi^{(i)}$ and $\chi^{(ii)}$ are given by

$$\chi = \frac{c_{11} - (c_{12} + c_{13})^2 + c_{11}(2c_{13} + c_{33})}{2c_{11}}. \tag{16}$$

Equation (15) defines the behavior of the equilibrium lattice constant relative to the relaxed core and shell lattice parameters. Figure 4 shows that the analytical functions are in good agreement with the numerical results, confirming that Eq. (15) is an appropriate approximation for the equilibrium lattice constant.

B. Partial relaxation via dislocation formation

The insertion of an edge dislocation at the core-shell interface can allow partial relaxation of lattice mismatch strain but will also contribute a strain field associated with the dislocation itself. In order to determine the energetics associated with these phenomena, it is necessary to identify the types of dislocations that are likely to form. This is done by first considering dislocations that are known to be stable in a given crystal structure and, from them, selecting those dislocations that will relieve lattice mismatch strain in the coaxial nanowire geometry. The two types of dislocations considered for the wurtzite [0001] structure are shown in Fig. 5.

A pure edge dislocation along the [0001] direction with Burgers vector in the $\langle 11\bar{2}0\rangle$, as shown in Fig. 5(a), is expected to be stable and relieve strain in the cross section of

the nanowire. Such dislocations have been observed in planar nitride films.[17] The strain energy associated with this type of dislocation is [18]

$$U_{\text{line}} = n_{\text{line}} 2\pi r L \left[\frac{c_{11}^{(ii)} - c_{12}^{(ii)}}{2c_{11}^{(ii)}} \right] \frac{{b_{\text{line}}}^2}{4\pi} \log\left(\frac{4h}{b_{\text{line}}} \right), \tag{17}$$

where n_{line} refers to the dislocation line density per unit length about the circumference of the heterointerface and b_{line} refers to the magnitude of the Burgers vector for such a dislocation. In this expression the dislocation is assumed to be located at the heterointerface, as shown in Fig. 5(a), and the strain field is assumed to terminate at the free surface of the nanowire system. Although the strain field generated by the dislocation will exist in both the core and shell materials, c_{ij} values are arbitrarily chosen to be those for the shell; this is reasonable since in most viable heterojunction material systems $c_{ij}^{(i)}$ and $c_{ij}^{(\text{ii})}$ are sufficiently similar that the choice between them will not significantly impact the final calculation. The magnitude of b_{line} is expected to be that of the equilibrium lattice constant a.[19]

Stable dislocations with Burgers vectors in the [0001] direction can also form in the wurtzite crystal structure.[18] If an edge dislocation loop with such a Burgers vector should form around the core, as shown in Fig. 5(b), some longitudinal strain in the wire would be relieved. Given that edge dislocations with such a Burgers vector are not observed in the planar case, we do not expect these dislocations to play a major role in coaxial structures but include it for completeness. The strain energy associated with such a dislocation loop is [18]

$$U_{\text{loop}} = n_{\text{loop}} L 2\pi r [c_{13}^{(ii)} + \sqrt{c_{11}^{(ii)} c_{33}^{(ii)}}] \sqrt{\frac{c_{44}^{(ii)} [\sqrt{c_{11}^{(ii)} c_{33}^{(ii)}} - c_{13}^{(ii)}]}{c_{11}^{(ii)} [c_{13}^{(ii)} + 2c_{44}^{(ii)} + \sqrt{c_{11}^{(ii)} c_{33}^{(ii)}}]}} \frac{{b_{\text{loop}}}^2}{4\pi} \times \log\left(\frac{32r}{b_{\text{loop}}} - 1 \right), \tag{18}$$

where n_{loop} refers to the dislocation loop density per unit length along the z axis of the wire and b_{loop} refers to the magnitude of the Burgers vector, which is assumed to be that of the equilibrium lattice constant c.

In examining the energetics of a dislocation at the interface, it is necessary to consider not only the strain field associated with the dislocation itself but also the lattice relaxation that is expected to occur with the inclusion of a dislocation. For planar thin films grown on bulk substrates, the one-dimensional lattice strain including relaxation due to dislocation formation is given by [14]

$$f_{\text{film}} = \frac{a_{\text{substrate}} - a_{\text{film}}}{a_{\text{film}}} - nb, \tag{19}$$

where $a_{\text{substrate}}$ represents the strained lattice constant of the film, a_{film} represents the relaxed lattice constant of the film, n refers to the line dislocation density per unit length, and b refers to the edge component of the dislocation Burgers vector. The lattice relaxation term nb accounts for the film relaxation due to the formation of dislocations at the heterointerface. The system described by Eq. (19) assumes that all strain will be in the film, and thus only relaxation in the film is considered.

In the case of the coaxial nanowire structures, strain will be distributed between the core and the shell. The formation of an edge dislocation at the interface will result in the insertion of an extra plane of atoms in the system. This will change the strain constraint in both core and shell materials since the two are interdependent. Because the system will tend to minimize total strain energy, the more heavily strained material will receive the bulk of the lattice relaxation that occurs. It is therefore necessary to distribute the lattice relaxation term between the core and shell while incorporating it into the lattice strain expressions. The resulting strain expressions are then

$$f_a^{(i)} = \frac{a - a^{(i)}}{a^{(i)}} - \left[\frac{a^{(i)} - a}{|a^{(i)} - a^{(ii)}|} \right] n_{\text{line}} b_{\text{line}}, \tag{20}$$

$$f_a^{(ii)} = \frac{a - a^{(ii)}}{a^{(ii)}} - \left[\frac{a - a^{(ii)}}{|a^{(i)} - a^{(ii)}|} \right] n_{\text{line}} b_{\text{line}}, \tag{21}$$

$$f_c^{(i)} = \frac{c - c^{(i)}}{c^{(i)}} - \left[\frac{c^{(i)} - c}{|c^{(i)} - c^{(ii)}|} \right] n_{\text{loop}} b_{\text{loop}}, \tag{22}$$

$$f_c^{(ii)} = \frac{c - c^{(ii)}}{c^{(ii)}} - \left[\frac{c - c^{(ii)}}{|c^{(i)} - c^{(ii)}|} \right] n_{\text{loop}} b_{\text{loop}}. \tag{23}$$

These expressions resemble Eq. (19) except that the lattice relaxation term is now divided between the core and shell. Equations (20)–(23) model the effect described earlier by using the equilibrium lattice constant and the relaxed lattice constant values to apportion the relaxation term according to the relative amounts of strain present in the core and shell materials. Numerical computations were carried out to minimize the total energy in the system with respect to the division of the strain relaxation term. The results of these calculations were found to be nearly identical to the functions used in Eqs. (20)–(23) confirming that the equilibrium lattice constant can be used to estimate the distribution of strain relaxation between the core and shell.

C. Critical geometry calculation

The total strain energy in the system is the sum of the lattice mismatch strain energy in the core and shell as well as the strain energy resulting from the strain fields of the two types of edge dislocations discussed above. The expression for the total strain energy including dislocations is therefore

$$U_{\text{tot}} = U^{(i)} + U^{(ii)} + U_{\text{line}} + U_{\text{loop}}, \tag{24}$$

where $U^{(i)}$ and $U^{(ii)}$ are calculated using Eqs.(11), (12), and (20)–(23). To determine the dimensions at which coherence is lost, it is necessary to determine the geometric limits at which it will become energetically favorable to include a dislocation. Mathematically this is done by evaluating $\partial U_{\text{tot}} / \partial n|_{n=0}$ and determining the dimensions for which this function changes from positive to negative.[14] This critical geometry analysis is carried out separately for line dislocations and loop dislocations.

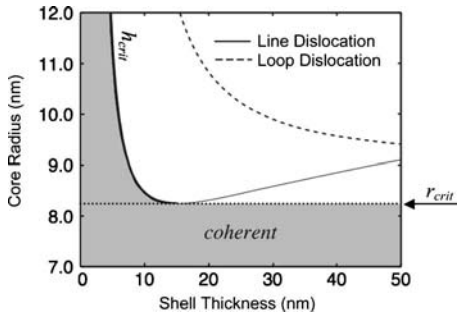

FIG. 6. Plot of the critical dimensions calculated for a coaxial nanowire structure comprised of a GaN core and $Al_{0.5}Ga_{0.5}N$ shell. The shaded region of the plot shows all possible strained coherent geometries, which are quantified by a critical core radius r_{crit} and the critical shell thickness curve h_{crit}.

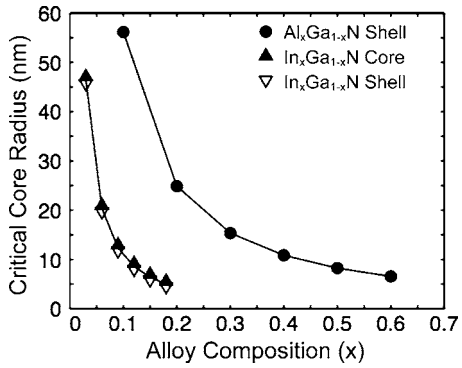

FIG. 7. Plot of the critical core radius for nitride nanowire heterostructures. The structures considered are comprised of a GaN core with $Al_xGa_{1-x}N$ shell (●), $In_xGa_{1-x}N$ core with GaN shell (▲), and GaN core with $In_xGa_{1-x}N$ shell (▽).

Such an analysis will determine the dimensions at which sufficient strain energy will be relieved by the insertion of a single dislocation to make up for the energy cost of inserting the dislocation. However, it does not take into account the energetic effects of interactions between dislocations, which are expected to be significant for nanoscale structures, and thus is only valid at the critical dimensions at which the first dislocation forms.

III. RESULTS AND DISCUSSION

Figure 6 shows the complete results of a critical geometry calculation for a structure comprised of a GaN core and an $Al_{0.5}Ga_{0.5}N$ shell. The solid and dashed curves show the calculated limiting dimensions for the formation of line dislocations and loop dislocations. The shaded portion of the plot shows the combination of core-shell dimensions that will yield coherently strained structures.

The solid curve in Fig 6 shows the limiting geometry for line dislocation formation. There is a critical core radius of 8.2 nm, below which a coaxial nanowire will be coherent regardless of shell thickness. Such a critical core radius exists because of the coaxial nanowire structure's ability to distribute strain between the core and shell. As the shell thickness increases, eventually all of the strain is passed to the core. Since the core volume is constant, the strain energy of the system will no longer change with shell thickness. If the core volume is sufficiently small, then the strain energy stored in the core will never be great enough to warrant the formation of a dislocation.

For structures with a core radius larger than the critical core radius, the solid curve in Fig. 6 will define a critical shell thickness for which it becomes energetically favorable to insert a line dislocation at the heterointerface. The positively sloped region of this curve (to the right of h_{crit} in Fig. 6) is a function of the assumption, used to calculate the dislocation strain energy U_{line}, that no other dislocations are present to terminate the dislocation strain field. Because a dislocation must have already formed in order to arrive at this region on the plot, the features of the curve in this region are not applicable in determining coherence.

The dashed curve in Fig. 6 shows the limiting geometry for loop dislocation formation. The position of this curve with respect to the line dislocation curve shows that coherence will always be lost through the formation of a line dislocation. Because the line dislocation has already formed in this region of the plot and the energetic interaction between dislocations is not taken into account, no other information can be extracted from the loop dislocation curve.

Hence, from Fig. 6 we are able to determine that the critical dimensions are defined by a critical core radius below which dislocations will never form and a critical shell thickness that is dependent on core radius. From the analysis we are also able to predict that coherence will likely be lost due to formation of a line dislocation oriented along the length of the wire.

Numerical calculations were also carried out for a number of other nitride structures as a function of alloy composition. Figure 7 shows critical core radii for structures comprised of GaN cores with $Al_xGa_{1-x}N$ shells, $In_xGa_{1-x}N$ cores with GaN shells, and GaN cores with $In_xGa_{1-x}N$ shells. Figures 8(a)–8(c) show the critical dimensions for these structures, respectively. These curves show the shell thickness at which the first line dislocation is expected to form for a given core radius. Figures 7 and 8 suggest that there are a variety of compositional and geometric choices that will yield coherent structures, giving device designers a flexibility that is typically not observed in planar thin film devices.

Few structures such as these have been fabricated and accurately characterized, and as a result limited data exist in the literature to directly determine the validity of this model. For increasing core radius, this model approaches the well-known theoretical calculation for planar thin films,[20–22] confirming that this model is consistent with accepted methods to determine critical thickness in thin film structures.

IV. CONCLUSION

In summary, we have developed a methodology to determine coherent geometries for coaxial nanowire heterostructures based on the well-known formalism used to determine the critical thickness in planar epitaxial growth. The unique geometry of the nanowire structure along with the volumetric similarity of the materials involved give rise to a number possible coherent structures for a given choice of materials,

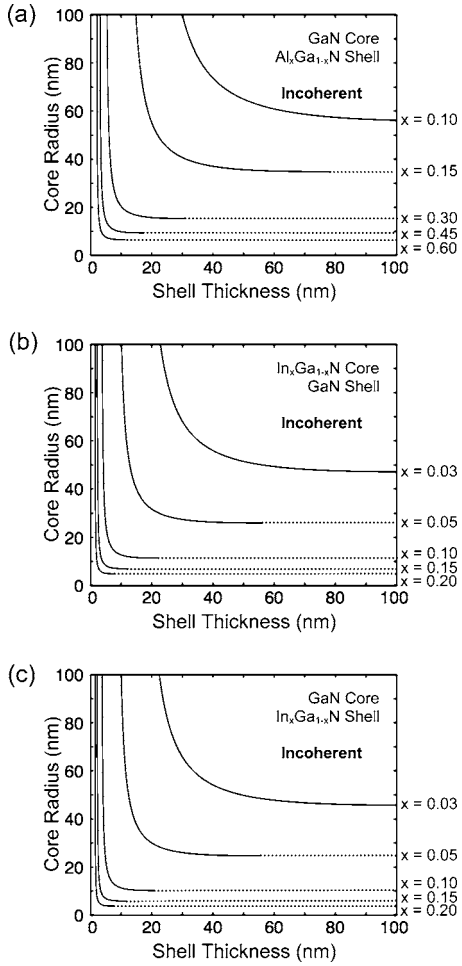

FIG. 8. Critical dimensions for various nitride nanowire heterojunctions. The structures are comprised of (a) GaN core with $Al_xGa_{1-x}N$ shell, (b) $In_xGa_{1-x}N$ core with GaN shell, and (c) GaN core with $In_xGa_{1-x}N$ shell.

which are quantified by a unique critical core radius and a critical shell thickness that is a function of the core radius. This flexibility is unique to nanowire structures and provides material and device engineers with increased flexibility in design not available in planar thin film heterostructures.

ACKNOWLEDGMENTS

Part of this work was supported by the National Science Foundation NIRT ECS-05069. One of the authors (S.R.) acknowledges financial support from a Cal(IT)^2 fellowship.

[1] M. Law, J. Goldberger, and P. Yang, Annu. Rev. Mater. Res. **34**, 83 (2004).
[2] Y. W. Heo, D. P. Norton, L. C. Tien, Y. Kwon, B. S. Kang, F. Ren, S. J. Pearton, and J. R. LaRoche, Mater. Sci. Eng., R. **47**, 1 (2004).
[3] F. Patolsky and C. M. Lieber, Mater. Today **8**, 20 (2005).
[4] B.-K. Kim, J.-J. Kim, J.-O. Lee, K.-J. Kong, H. J. Seo, and C. J. Lee, Phys. Rev. B **71**, 153313 (2005).
[5] L. J. Lauhon, M. S. Gudiksen, D. Wang, and C. M. Lieber, Nature (London) **420**, 57 (2002).
[6] Y. Zhang, R. E. Russo, and S. S. Mao, Appl. Phys. Lett. **87**, 043106 (2005).
[7] H.-J. Choi *et al.*, J. Phys. Chem. B **107**, 8721 (2003).
[8] O. Hayden, A. B. Greytak, and D. C. Bell, Adv. Mater. (Weinheim, Ger.) **17**, 701 (2005).
[9] R. Könenkamp, R. C. Word, and C. Schlegel, Appl. Phys. Lett. **85**, 6004 (2005).
[10] L. J. Lauhon, M. S. Gudiksen, and C. M. Lieber, Philos. Trans. R. Soc. London, Ser. A **362**, 1247 (2004).
[11] E. Ertekin, P. A. Greaney, D. C. Chrzan, and T. D. Sands, J. Appl. Phys. **97**, 114325 (2005).
[12] M. Yu. Gutkin, I. A. Ovid'ko, and A. G. Sheinerman, J. Phys.: Condens. Matter **12**, 5391 (2000).
[13] J. W. Matthews, J. Vac. Sci. Technol. **12**, 126 (1975).
[14] J. Y. Tsao, *Materials Fundamentals of Molecular Beam Epitaxy* (Academic, San Diego, 1993), pp. 151–168.
[15] J. F. Nye, *Physical Properties of Crystals* (Oxford University Press, Oxford, 1985), pp. 82–104, 131–142.
[16] O. Ambacher *et al.*, J. Phys.: Condens. Matter **14**, 3399 (2002).
[17] P. Cantu, F. Wu, P. Waltereit, S. Keller, A. E. Romanov, S. P. DenBaars, and J. S. Speck, J. Appl. Phys. **97**, 103534 (2005).
[18] J. P. Hirth and J. Lothe, *Theory of Dislocations* (McGraw-Hill, New York, 1968), pp. 29–56, 140–144, 254–265, 411–432.
[19] J. A. Floro, D. M. Follstaedt, P. Provencio, S. J. Hearne, and S. R. Lee, J. Appl. Phys. **96**, 7087 (2004).
[20] S. R. Lee, D. D. Koleske, K. C. Cross, J. A. Floro, K. E. Waldrip, A. T. Wise, and S. Mahajan, Appl. Phys. Lett. **85**, 6164 (2004).
[21] A. D. Bykhovski, B. L. Gelmont, and M. S. Shur, J. Appl. Phys. **81**, 6332 (1997).
[22] A. D. Bykhovski, B. L. Gelmont, and M. S. Shur, J. Appl. Phys. **78**, 3691 (1995).